Detection and Characterization of Bat Sarbecovirus Phylogenetically Related to SARS-CoV-2, Japan

Shin Murakami,[1] Tomoya Kitamura,[1] Jin Suzuki, Ryouta Sato, Toshiki Aoi, Marina Fujii, Hiromichi Matsugo, Haruhiko Kamiki, Hiroho Ishida, Akiko Takenaka-Uema, Masayuki Shimojima, Taisuke Horimoto

Epidemiology of bat *Betacoronavirus*, subgenus *Sarbecovirus* is largely unknown, especially outside China. We detected a sarbecovirus phylogenetically related to severe acute respiratory syndrome coronavirus 2 from *Rhinolophus cornutus* bats in Japan. The sarbecovirus' spike protein specifically recognizes angiotensin-converting enzyme 2 of *R. cornutus*, but not humans, as an entry receptor.

During the past 20 years, coronaviruses belonging to the genus *Betacoronavirus* have caused multiple human epidemic or pandemic diseases, including severe acute respiratory syndrome (SARS), Middle East respiratory syndrome (MERS), and coronavirus disease (COVID-19). Two viruses of the subgenus *Sarbecovirus* are severe acute respiratory syndrome coronavirus (SARS-CoV), which causes SARS, and SARS-CoV-2, which causes COVID-19. Although *Rhinolophus* spp. bats in Asia, Europe, and Africa are considered natural reservoirs of sarbecoviruses (*1*–*3*), the epidemiology and distribution of these viruses remain largely unknown, especially outside China. Previously, partial RNA-dependent RNA polymerase (RdRp) genes of betacoronaviruses were detected in little Japanese horseshoe bats (*Rhinolophus cornutus*) (*4*). However, limited sequence information left the genetic and virological properties unclear. We detected and determined the entire genome sequence of a bat sarbecovirus belonging to a phylogenetic clade that includes SARS-CoV-2 from *R. cornutus* bats in Japan. Further, we used a pseudotyped virus system to characterize an entry step of this virus into cells.

Author affiliations: The University of Tokyo, Tokyo, Japan (S. Murakami, T. Kitamura, M. Fujii, H. Matsugo, H. Kamiki, H. Ishida, A. Takenaka-Uema, T. Horimoto); Yamaguchi University, Yamaguchi, Japan (J. Suzuki); Iwate University, Iwate, Japan (R. Sato, T. Aoi); National Institute of Infectious Diseases, Tokyo, Japan (M. Shimojima)

DOI: https://doi.org/10.3201/eid2612.203386

The Study

R. cornutus is an endemic bat species in Japan and is found nationwide. These bats primarily inhabit caves and abandoned tunnels in the countryside during daytime and capture insects at night outside their roosts. *R. cornutus* bats often cohabit with other insectivorous bats, such as *R. ferrumequinum* or *Myotis macrodactylus*, and occasionally with wild animals, such as the masked palm civet (*Paguma larvata*), in their daytime roosts.

In 2013, we captured 4 *R. cornutus* bats in a cave in Iwate prefecture, Japan, and extracted RNA from fresh feces. Then, we used real-time reverse transcription PCR (rRT-PCR) to detect the partial RdRp gene of sarbecovirus from 2 samples by using a pair of primers designed to detect betacoronavirus. In 2020, we performed RNA sequencing and determined the full genome sequence of 1 sample, Rc-o319, which exhibited lower cycle threshold value by rRT-PCR.

We performed a BLAST (https://blast.ncbi.nlm.nih.gov/Blast.cgi) analysis of the full genome of Rc-o319, which showed Rc-o319 had the highest nucleotide homology to SARS-CoV-2 HKG/HKU-904a/2020 strain (GenBank accession no. MT365032) with a query cover of 96% and sequence identity of 81.47%. The maximum-likelihood analysis with sarbecoviruses demonstrated that the full genome and spike protein (S) gene of Rc-o319 were positioned within a specific clade that included SARS-CoV-2 (Figure 1, panels A, B). Amino acid sequences of open reading frame 1ab (ORF1ab) and S of Rc-o319 also were positioned within the SARS-CoV-2 clade (Figure 1 panels C and D). The phylogenetic trees maintained the same topology between ORF1ab and S, indicating that no recombination event occurred in Rc-0319, which was supported by similarity plot analysis (Appendix Figure 1, https://wwwnc.cdc.gov/EID/article/26/12/

[1]These authors contributed equally to this article.

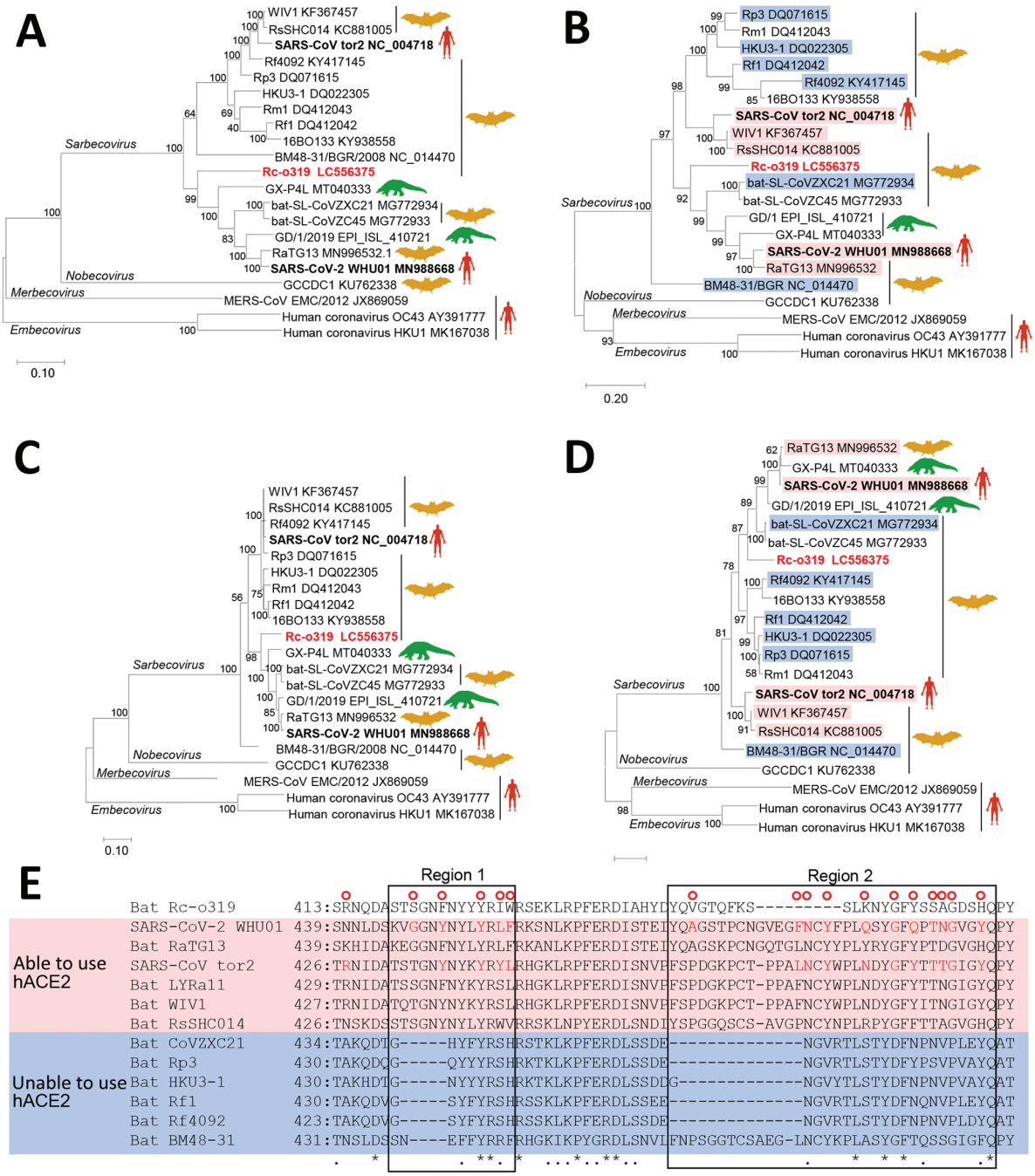

Figure 1. Phylogenetic analysis of sarbecovirus sequenced from little Japanese horseshoe bats (*Rhinolophus cornutus*) and genetically related to human SARS-CoV-2, Japan. A–D) Phylogenetic trees were generated by using maximum-likelihood analysis combined with 500 bootstrap replicates and show relationships between bat-, human-, and pangolin-derived sarbecoviruses. Phylogenetic trees are shown for nucleotide sequences of the full genome (A), the S protein gene and amino acid sequences (B), the ORF1ab (C), and the S protein (D). Red text indicates positions of Rc-o319, the sarbecovirus sequenced in this study. For panels B and D, magenta bands indicate viruses with S proteins that bind to human ACE2; blue bands indicate viruses with S proteins that do not bind to human ACE2. Bootstrap values are shown above and to the left of the major nodes. Scale bars indicate nucleotide or amino acid substitutions per site. E) Amino acid sequence alignment of the RBM of S proteins that are able or unable to bind to human ACE2. Amino acid residues of the RBM that contact human ACE2 of SARS-CoV-2 and SARS-CoV are indicated in the upper side by red circles. The 2 regions of S protein RBM known to interact with human ACE2 are indicated by boxes labeled region 1 and region 2. ACE2, angiotensin-converting enzyme 2; hACE2, human angiotensin-converting enzyme 2; ORF1ab, open reading frame 1ab; RBM, receptor-binding motif; S, spike protein; SARS-CoV, severe acute respiratory syndrome coronavirus; SARS-CoV-2, severe acute respiratory syndrome coronavirus 2.

20-3386-App1.pdf). The nucleotide and amino acid sequences of Rc-o319 were more homologous to those of viruses belonging to SARS-CoV-2 clade than the SARS-CoV clade (Table). These data suggest that Rc-o319 genetically is related to SARS-CoV-2.

To gain insight into the zoonotic potential of Rc-o319, we focused on angiotensin-converting enzyme 2 (ACE2) receptor binding motif (RBM) of the S protein (Figure 1, panel E). RBM has 2 regions (1 and 2); both are essential to human ACE2 (hACE2) recognition (*5*,*6*). Several S proteins of bat-origin sarbecoviruses that lack the ability to bind the hACE2 contain amino acid deletions in both regions (Figure 1, panel E) (*5*). However, the RBM of Rc-o319 S is unique because it has 9 aa deletions in region 2 only, which was not observed in other bat sarbecoviruses. Of note, most residues that contact hACE2, which were detected in the S protein of SARS-CoV-2 and SARS-CoV, were different or missing in the S protein of Rc-o319. Thus, current data do not enable inference for whether the Rc-o319 can use hACE2 as a cell entry receptor.

To evaluate the potential of ACE2 as a receptor for Rc-o319, we adopted a pseudotyped vesicular stomatitis virus (VSV) system, in which VSV glycoprotein envelope (G) gene is replaced by green fluorescent protein (GFP) gene. We generated VSV pseudotyped with S proteins of Rc-o319 (VSV-Rc-o319), SARS-CoV (VSV-SARS), SARS-CoV-2 (VSV-SARS-2), or VSV-G (VSV-VSV-G) in human embryonic kidney 293T (HEK293T) cells. We also constructed ACE2 expression plasmids from hACE2, *R. ferrumequinum* bats (Rf-ACE2), and *R. sinicus* bats (Rs-ACE2). *R. ferrumequinum* is another bat species inhabiting in Japan, and *R. sinicus* bats are a major host reservoir of bat sarbecoviruses. We also prepared a chimeric bat ACE2 from *R. cornutus* and *R. ferrumequinum* bats, Rc/Rf chimera, which has the N terminus of S protein interaction domain of Rc-ACE2 and the remaining region from Rf-ACE2 (Appendix Figure 2). The HEK293T cells expressing Rc-ACE2, Rf-ACE2, Rs-ACE2, Rc/Rf-ACE2, or hACE2 were produced by transfecting each ACE2-expression plasmid (Appendix Figure 3) and inoculating them with pseudotyped VSVs; their infectivity was titrated by counting GFP-positive cells at 20 hours postinfection (Figure 2). Our results showed that VSV-Rc-o319 infected Rc-ACE2– and Rc/Rf-ACE2–expressing cells, but not Rf-ACE2–, Rs-ACE2–, or hACE2–expressing cells or control cells transfected with empty vector plasmid. In contrast, VSV-SARS and VSV-SARS-2 more effectively infected hACE2-expressing cells than bat ACE2–expressing cells and control cells. VSV-VSV-G infected all tested cells to comparable levels, confirming ACE2-independent infectivity of VSV. These results suggest high specificity of ACE2 receptor between sarbecovirus and host cells and possibly a limited zoonotic potential of Rc-o319 in terms of cell receptor usage without adaptation to humans.

We next analyzed the membrane fusion step of Rc-o319 S. A previous study showed that human sarbecovirus S protein was proteolytically activated by cellular transmembrane serine protease 2 (TMPRSS2), in vitro and in vivo, inducing efficient virus-cell membrane fusion at the cell surface (*7*). We prepared a fusion assay, in which HEK293T cells were cotransfected with S-expression plasmid of Rc-o319, SARS-CoV, or SARS-CoV-2 and Rc-ACE2–, Rf-ACE2–, Rs-ACE2–, or hACE2-expression plasmid, together with fluorescent reporter Venus-expression plasmid with and without TMPRSS2-expression plasmid, and incubated for 24 h to assess syncytium formation. We observed that the S protein

Table. Identities of nucleotide and amino acid sequences of genome, genes, and proteins to representative sarbecoviruses used to investigate sarbecovirus Rc-o319 detected in bats, Japan

Virus	Entire genome	ORF1ab	S	ORF3a	E	M	ORF6	ORF7a	ORF7b	ORF8	N	ORF10
						Nucleotide %						
SARS-CoV-2	81.5	80.0	73.0	83.2	97.4	86.6	86.6	78.4	77.3	53.3	88.3	94.9
RaTG13	81.2	79.8	73.3	83.9	96.9	85.4	87.1	77.4	78.0	53.0	87.8	94.0
pangolin/P4L	80.4	79.8	72.5	83.5	97.8	85.5	85.5	74.5	–	53.2	86.8	91.5
CoVZXC21	80.4	80.2	72.5	79.9	96.1	86.0	83.3	75.1	–	50.8	85.9	53.9
SARS-CoV-1	81.0	78.8	73.6	76.6	93.1	87.0	77.1	73.4	74.8	–	86.1	63.3
Rf1	80.6	78.7	70.9	75.1	92.6	85.8	78.8	72.2	75.6	68.6	84.9	63.3
BM48–31	79.6	77.4	69.3	70.4	90.5	80.6	61.3	65.1	57.9	–	77.0	64.1
						Amino acid, %						
SARS-CoV-2	NA	88.2	76.7	87.0	98.7	91.0	83.6	73.8	69.8	27.5	89.5	87.2
RaTG13	NA	88.1	77.6	86.6	98.7	91.0	83.6	73.0	72.1	28.2	89.7	84.6
pangolin/P4L	NA	88.2	76.9	86.2	98.7	91.0	80.3	68.9	–	28.8	89.2	79.5
CoVZXC21	NA	87.9	75.5	83.3	98.7	91.4	77.1	68.9	–	20.5	88.1	28.2
SARS-CoV-1	NA	85.9	75.2	72.5	93.4	97.7	66.7	69.7	68.2	–	88.9	59.0
Rf1	NA	85.5	73.6	69.6	92.1	94.1	66.7	68.0	72.7	66.7	87.4	59.0
BM48–31	NA	83.7	71.9	64.5	93.4	88.1	48.5	52.5	58.1	–	85.9	61.5

*NA, not available; ORF, open reading frame; –, no ORFs found.

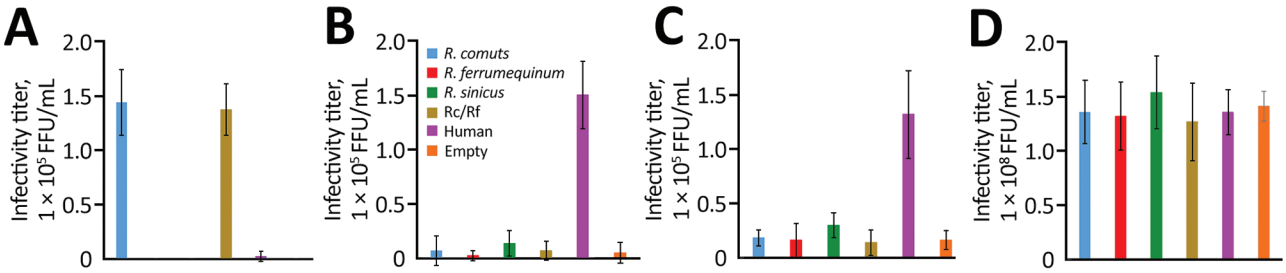

Figure 2. Infectivity titers of sarbecoviruses from bats and humans used to investigate bat sarbecovirus Rc-o319, which is genetically related to human SARS-CoV-2, Japan. Cells expressing each host-origin angiotensin-converting enzyme 2 were inoculated with VSV pseudotyped with spike proteins of Rc-o319 (A), SARS-CoV (B), SARS-CoV-2 (C), or glycoprotein of VSV (D). At 20 hours postinfection, GFP-positive cells were counted and the infectivity titers were calculated. Error bars indicate SDs from 3 independent experiments. CoV, coronavirus; GFP, green fluorescent protein; Rc/Rf, chimera of *Rhinolophus cornutus* and *R. ferrumequinum*; SARS, severe acute respiratory syndrome; VSV, vesicular stomatitis virus.

of SARS-CoV and SARS-CoV-2 required both hACE2 and TMPRSS2 for fusion activity (Appendix Figure 4), confirming the previous findings (*7*,*8*). In contrast, the S protein of Rc-o319 induced cell fusion only in Rc-ACE2–expressing cells, both in the presence and absence of TMPRSS2. These results suggest that unlike human sarbecoviruses, Rc-o319 uses Rc-ACE2 as a functional receptor, leading to membrane fusion independent of S-cleavage by TMPRSS2.

Conclusions

Among *R. cornutus* bats in Japan, we detected sarbecovirus Rc-o319, which is phylogenetically positioned in the same clade as SARS-CoV-2. Sarbecoviruses belonging to this clade previously were detected from other *Rhinolophus* spp. bats and pangolins (family Manidae) in China and could have played a role in the emergence of SARS-CoV-2 (*9*–*11*). We provide a hypothesis that a bat sarbecovirus with zoonotic potential might exist even outside China, because *Rhinolophus* spp. bats inhabit Asia, Europe, and Africa (*12*).

Receptor usage is one factor for cross-species transmission of viruses. Unlike a previous report that showed that some bat SARS-CoV–related viruses could use human and civet ACE2 and *R. sinicus* ACE2 as entry receptors (*5*,*13*,*14*), VSV-Rc-o319 was found to use only homologous Rc-ACE2, which arguably suggests that Rc-o319 and its related viruses might not jump the species barrier easily and cause infection. However, Rc-o319 and its related viruses could be transmitted accidentally from *R. cornutus* bats to cohabitant animals, such as civets, which are potential intermediate hosts for human infection (*15*). Therefore, further epidemiologic surveillance of bat betacoronaviruses, including evaluation of their zoonotic potential, is essential because betacoronaviruses that caused SARS, MERS, and COVID-19 outbreaks in humans during the past 20 years likely originated from bat betacoronaviruses.

S.M. is supported by a Kakenhi Grant-in-Aid for Challenging Research (Exploratory) from the Japan Society for the Promotion of Science (grant no. 17K19319).

About the Author

Dr. Murakami is an associate professor at the Graduate School of Agricultural and Life Sciences, University of Tokyo, Tokyo, Japan. His research interests include epidemiologic and molecular biological studies of animal viruses, including coronaviruses and influenza viruses.

References

1. Drexler JF, Gloza-Rausch F, Glende J, Corman VM, Muth D, Goettsche M, et al. Genomic characterization of severe acute respiratory syndrome-related coronavirus in European bats and classification of coronaviruses based on partial RNA-dependent RNA polymerase gene sequences. J Virol. 2010;84:11336–49. https://doi.org/10.1128/JVI.00650-10
2. Hu B, Zeng LP, Yang XL, Ge XY, Zhang W, Li B, et al. Discovery of a rich gene pool of bat SARS-related coronaviruses provides new insights into the origin of SARS coronavirus. PLoS Pathog. 2017;13:e1006698. https://doi.org/10.1371/journal.ppat.1006698
3. Tao Y, Tong S. Complete genome sequence of a severe acute respiratory syndrome-related coronavirus from Kenyan bats. Microbiol Resour Announc. 2019 8(28):e00548–19. https://doi.org/0.1128/MRA.00548-19
4. Suzuki J, Sato R, Kobayashi T, Aoi T, Harasawa R. Group B betacoronavirus in rhinolophid bats, Japan. J Vet Med Sci. 2014;76:1267–9. https://doi.org/10.1292/jvms.14-0012
5. Letko M, Marzi A, Munster V. Functional assessment of cell entry and receptor usage for SARS-CoV-2 and other lineage B betacoronaviruses. Nat Microbiol. 2020;5:562–9. https://doi.org/10.1038/s41564-020-0688-y
6. Lan J, Ge J, Yu J, Shan S, Zhou H, Fan S, et al. Structure of the SARS-CoV-2 spike receptor-binding domain bound to the

ACE2 receptor. Nature. 2020;581:215–20. https://doi.org/10.1038/s41586-020-2180-5
7. Glowacka I, Bertram S, Müller MA, Allen P, Soilleux E, Pfefferle S, et al. Evidence that TMPRSS2 activates the severe acute respiratory syndrome coronavirus spike protein for membrane fusion and reduces viral control by the humoral immune response. J Virol. 2011;85:4122–34. https://doi.org/10.1128/JVI.02232-10
8. Yamamoto M, Kiso M, Sakai-Tagawa Y, Iwatsuki-Horimoto K, Imai M, Takeda M, et al. The anticoagulant nafamostat potently inhibits SARS-CoV-2 S protein-mediated fusion in a cell fusion assay system and viral infection in vitro in a cell-type-dependent manner. Viruses. 2020;12:E629. https://doi.org/10.3390/v12060629
9. Zhou P, Yang XL, Wang XG, Hu B, Zhang L, Zhang W, et al. A pneumonia outbreak associated with a new coronavirus of probable bat origin. Nature. 2020;579:270–3. https://doi.org/10.1038/s41586-020-2012-7
10. Lau SKP, Luk HKH, Wong ACP, Li KSM, Zhu L, He Z, et al. Possible bat origin of severe acute respiratory syndrome coronavirus 2. Emerg Infect Dis. 2020;26:1542–7. https://doi.org/10.3201/eid2607.200092
11. Zhang T, Wu Q, Zhang Z. Probable pangolin origin of SARS-CoV-2 associated with the COVID-19 outbreak. Curr Biol. 2020;30:1346–51.e2. https://doi.org/10.1016/j.cub.2020.03.022
12. Stoffberg S, Jacobs DS, Mackie IJ, Matthee CA. Molecular phylogenetics and historical biogeography of Rhinolophus bats. Mol Phylogenet Evol. 2010;54:1–9. https://doi.org/10.1016/j.ympev.2009.09.021
13. Ge XY, Li JL, Yang XL, Chmura AA, Zhu G, Epstein JH, et al. Isolation and characterization of a bat SARS-like coronavirus that uses the ACE2 receptor. Nature. 2013;503:535–8. https://doi.org/10.1038/nature12711
14. Yang XL, Hu B, Wang B, Wang MN, Zhang Q, Zhang W, et al. Isolation and characterization of a novel bat coronavirus closely related to the direct progenitor of severe acute respiratory syndrome coronavirus. J Virol. 2015;90:3253–6. https://doi.org/10.1128/JVI.02582-15
15. Guan Y, Zheng BJ, He YQ, Liu XL, Zhuang ZX, Cheung CL, et al. Isolation and characterization of viruses related to the SARS coronavirus from animals in southern China. Science. 2003;302:276–8. https://doi.org/10.1126/science.1087139

Address for correspondence: Shin Murakami or Taisuke Horimoto, Department of Veterinary Microbiology, Graduate School of Agricultural and Life Sciences, University of T okyo, 1-1-1 Yayoi, Bunkyo-ku, Tokyo 113-8657, Japan; email: amurakam@mail.ecc.u-tokyo.ac.jp or ahorimo@mail.ecc.u-tokyo.ac.jp

EID Podcast
Meningitis in U.S. Colleges

The number of reported outbreaks of meningococcal disease at U.S. universities has increased in recent years, despite the availability of vaccines. So why are college students still at increased risk for this potentially deadly disease?

In this EID podcast, Dr. Heidi Soeters, a CDC epidemiologist, discusses the prevalence of meningitis at U.S. universities.

Visit our website to listen:
https://tools.cdc.gov/medialibrary/index.aspx#/media/id/397588
EMERGING INFECTIOUS DISEASES®

Article DOI: https://doi.org/eid2612/203386

Detection and Characterization of Bat Sarbecovirus Phylogenetically Related to SARS-CoV-2, Japan

Appendix

Additional Methods

Sample Collection

We captured 4 *Rhinolophus cornutus* bats in a cave in Iwate prefecture, Japan, in 2013, with permission from the prefectural local government. Each bat was kept in a separate plastic bag. Fresh feces samples were collected, transferred into tubes containing sterilized saline, and frozen in dry ice. We released the bats after feces collection.

Reverse Transcription-PCR

RNA was extracted from the feces samples using an RNeasy PowerMicrobiome Kit (QIAGEN, https://www.qiagen.com). Next, we detected the partial RNA-dependent RNA polymerase (RdRp) gene of sarbecovirus in 2 samples by real-time reverse transcription-PCR by using RNA-direct SYBR Green Realtime PCR Master Mix (TOYOBO, https://www.toyobo-global.com) and a pair of primers (5′-CATATGCAGTAGTGGCATCA-3′ and 5′-GCTGTAACTTGTCACATCGT-3′) that were designed based on a previous report (*1*).

Next-Generation Sequencing

A cDNA library was prepared from RNA extracted from the feces sample by using the SMARTer Stranded RNA-Seq Kit (Takara-Bio, https://www.takarabio.com). The library

was sequenced by using a NovaSeq 6000 (Illumina, https://www.illumina.com) sequencer. The read sequences were mapped on RaTG13 (GenBank accession no. MN996532), and the Rc-o319 sequence was determined by using CLC genomic workbench version 8.0.1 (QIAGEN, https://www.qiagen.com) software. The sequence was deposited in GenBank (accession no. LC556375).

Phylogenetic Analysis

The nucleotide and amino acid (aa) sequences of sarbecoviruses were aligned by using ClustalW version 2.1(Clustal, https://www.clustal.org). Phylogenetic trees were constructed by performing maximum-likelihood analysis with MEGA version X (*2*), in combination with 500 bootstrap replicates.

Plasmids

We cloned the spike protein (S) genes of Rc-o319 and severe acute respiratory syndrome coronavirus 2 (SARS-CoV-2; 2019-nCoV/Japan/AI/I-004/2020, GenBank accession no. LC521925), with a 19–aa deletion at the C-terminus (pCAGGS-o319-S-del19), into protein expression pCAGGS vectors (pCAGGS-SARS-CoV-2-del19). Earlier reports have suggested that this deletion leads to the efficient production of vesicular stomatitis virus (VSV) pseudotyped with the S gene of SARS-CoV (*3*). We used the SARS-CoV S gene expression plasmid pKS-SARS-St19 (*3*) and the vesicular stomatitis Indiana virus glycoprotein (G)-expression plasmid pCAGGS-VSV-G (*4*). We also constructed angiotensin-converting enzyme 2 (ACE2)-expression plasmids derived from humans (hACE2; GenBank accession no. NM_001371415), greater horseshoe bats (*R. ferrumequinum*) (Rf-ACE2; GenBank accession no. AB297479), and Chinese rufous horseshoe bats (*R. sinicus*) (Rs-ACE2; GenBank accession no. KC881004). The hACE2 cDNA was amplified from RNA isolated from Caco-2 cells by RT-PCR, and the Rf-ACE2 and Rs-ACE2 genes were

artificially synthesized and cloned into pCAGGS plasmids (pCAGGS-hACE2, pCAGGS-Rs-ACE2, or pCAGGS-Rf-ACE2, respectively).

Because fresh RNA samples from *R. cornutus* bats were not available, the ACE2 gene of *R. cornutus* (Rc-ACE2) was amplified from the exon regions of genomic DNA extracted from the kidney of a bat carcass (GenBank accession no. LC564973) and cloned into the pCAGGS vector that was designated as pCAGGS-Rc-ACE2. We also prepared a chimeric bat ACE2 (referred to as Rc/Rf chimera), which consisted of the S interaction domain of Rc-ACE2 (aa positions 15–116) and the remaining region from Rf-ACE2, to form the expression plasmid pCAGGS-Rc/Rf-ACE2.

Western Blot Analysis

HEK293T cells were transfected with pCAGGS-RcACE2, pCAGGS-hACE2, pCAGGS-RfACE2, pCAGGS-RsACE2, pCAGGS-Rc/RfACE2, or empty pCAGGS vectors. One day after transfection, the cells were lysed with SDS sample buffer and subjected to western blotting by using rabbit anti-ACE2 antibody (Abcam, https://www.abcam.com).

Production of VSV-Pseudotyped Virus

VSVΔG*-GFP, which expresses a GFP reporter gene instead of the viral G gene, was used to produce VSV pseudotyped with S genes from sarbecoviruses, as described in earlier reports (*3,5*). HEK293T cells seeded on 6-well plates were transfected with 2 μg of either pCAGGS-o319-S-del19, pCAGGS-SARS-CoV-2-del19, pKS-SARS-St19, or control pCAGGS-VSV-G. At 24 h post-transfection, the cells were infected with VSVΔG*-GFP and incubated for 24 h. The culture fluid was collected, centrifuged, filtered through a 0.45-μm filter to remove cells and cell debris, and stored at −80°C until use. The pseudotyped viruses with Rc-o319 S were designated as VSV-Rc-o319, for SARS-CoV S were designated VSV-SARS, for SARS-CoV-2 S were designated VSV-SARS-2, and for VSV-G were designated VSV-VSV-G. The viruses pseudotyped with sarbecovirus S proteins were incubated with the

anti-VSV-G neutralizing antibody I1 (*6*) for 30 min at 21°C to eliminate the remaining VSVΔG*-GFP.

Cell Entry Assay

HEK293T cells seeded on 24-well plates were transfected with 0.5 μg of either pCAGGS-Rc-ACE2, pCAGGS-Rf-ACE2, pCAGGS-Rs-ACE2, pCAGGS-Rc/Rf-ACE2, pCAGGS-hACE2, or control empty pCAGGS plasmids, and incubated for 24 h. Each pseudotyped virus (200 μL) was used to inoculate each ACE2-expression cell culture. After incubation at 37°C for 1 h, the cells were washed once with Opti-MEM (Thermo Fisher Scientific, https://www.thermofisher.com) and incubated with Opti-MEM at 37°C for 20 h. The number of GFP-positive cells within 1 microscopic field (3.1 mm^2) was counted under an Axio Vert.A1 fluorescent microscope (Carl Zeiss, https://www.zeiss.com). The virus titers were determined as the number of GFP-positive cells per well in a 24-well plate (1.9 cm^2), calculated for 5 microscopic fields. The virus titers are expressed in terms of the average values with standard deviations from 3 independent experiments.

Cell Fusion Assay

HEK293T cells were cotransfected with 1 of the S-expression plasmids (pCAGGS-o319-S-del19, pCAGGS-SARS-CoV-2-del19, or pKS-SARS-St19) and 1 of the ACE2-expression plasmids (pCAGGS-Rc-ACE2, pCAGGS-Rf-ACE2, pCAGGS-Rs-ACE2, or pCAGGS-hACE2), with or without the TMPRSS2-expression plasmid, and a fluorescent reporter Venus-expression plasmid (*7*) for the convenient visualization of fused cells under a fluorescence microscope. After transfection, the cells were incubated at 37°C for 24 h. The fused cells were observed under an Axio Vert.A1 fluorescence microscope (Carl Zeiss). As a control, we confirmed that no appreciable syncytium was observed in HEK293T cells transfected with each S-expression plasmid, which indicates that endogeneous hACE2 in these cells did not affect the results of the cell fusion assay.

References

1. Suzuki J, Sato R, Kobayashi T, Aoi T, Harasawa R. Group B betacoronavirus in rhinolophid bats, Japan. J Vet Med Sci. 2014;76:1267–9. PubMed https://doi.org/10.1292/jvms.14-0012

2. Kumar S, Stecher G, Li M, Knyaz C, Tamura K. MEGA X: Molecular evolutionary genetics analysis across computing platforms. Mol Biol Evol. 2018;35:1547–9. PubMed https://doi.org/10.1093/molbev/msy096

3. Fukushi S, Mizutani T, Saijo M, Matsuyama S, Miyajima N, Taguchi F, et al. Vesicular stomatitis virus pseudotyped with severe acute respiratory syndrome coronavirus spike protein. J Gen Virol. 2005;86:2269–74. PubMed https://doi.org/10.1099/vir.0.80955-0

4. Murakami S, Horimoto T, Mai Q, Nidom CA, Chen H, Muramoto Y, et al. Growth determinants for H5N1 influenza vaccine seed viruses in MDCK cells. J Virol. 2008;82:10502–9. PubMed https://doi.org/10.1128/JVI.00970-08

5. Takada A, Robison C, Goto H, Sanchez A, Murti KG, Whitt MA, et al. A system for functional analysis of Ebola virus glycoprotein. Proc Natl Acad Sci U S A. 1997;94:14764–9. PubMed https://doi.org/10.1073/pnas.94.26.14764

6. Iwasa A, Shimojima M, Kawaoka Y. sGP serves as a structural protein in Ebola virus infection. J Infect Dis. 2011;204:S897–903. PubMed https://doi.org/10.1093/infdis/jir313

7. Nagai T, Ibata K, Park ES, Kubota M, Mikoshiba K, Miyawaki A. A variant of yellow fluorescent protein with fast and efficient maturation for cell-biological applications. Nat Biotechnol. 2002;20:87–90. PubMed https://doi.org/10.1038/nbt0102-87

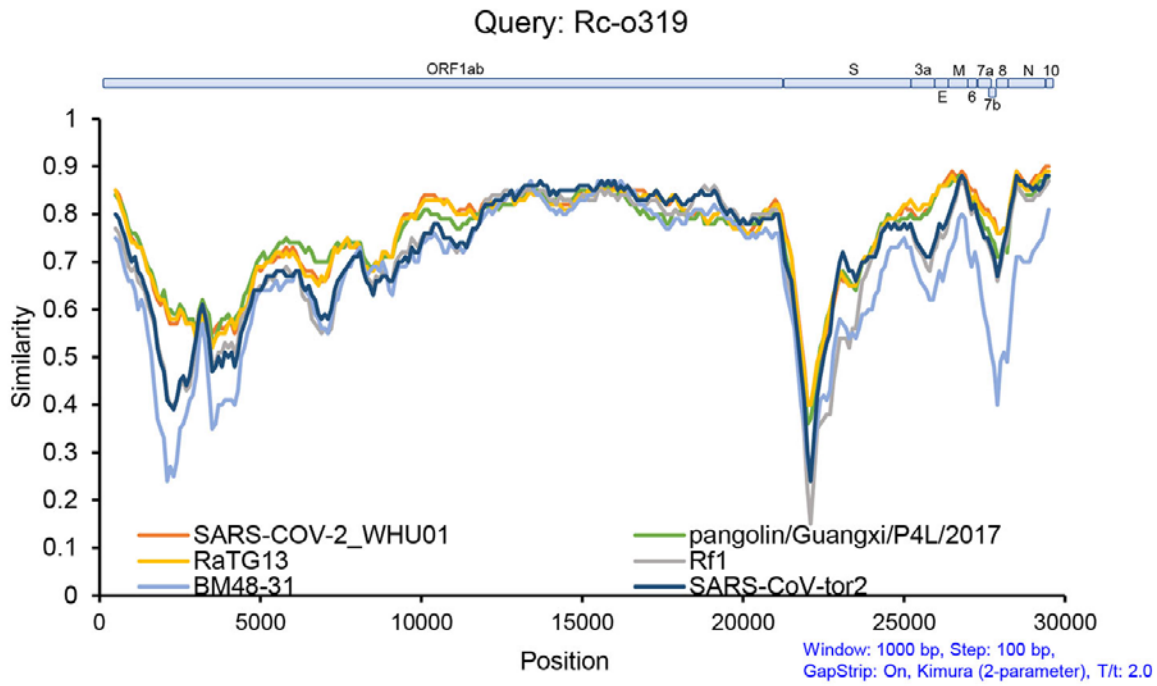

Appendix Figure 1. Similarity plot analysis of sarbecovirus Rc-o319 sequenced from little Japanese horseshoe bats (*Rhinolophus cornutus*) and genetically related to human SARS-CoV-2, Japan. Full-length genome sequence of Rc-o319 was used as query. Representative sequences from sarbecoviruses were used as references. ORF1ab, open reading frame 1ab; SARS-CoV-2, severe acute respiratory syndrome coronavirus 2.

```
R.cornutus        1:MSGSSWLLLSLVAVTAAQSTTEDEAKKFLNDFNSEAENLTYQSSLASWDYNTNISDENVQ 60
R.ferrumequinum   1:MSGSSWLLLSLVAVTAAQSTTEDLAKKFLDDFNSEAENLSHQSSLASWEYNTNISDENVQ 60
R.sinicus         1:MSGSSWLLLSLVAVTTAQSTTEDEAKMFLDKFNTKAEDLSHQSSLASWDYNTNINDENVQ 60
human             1:MSSSSWLLLSLVAVTAAQSTIEEQAKTFLDKFNHEAEDLFYQSSLASWNYNTNITEENVQ 60
                    **.************.****.*. ** **. ** .** *  ******* ***** .****

R.cornutus       61:KMDEAGAKWSAFYEEQSKIAKNYPLEEIQTDIVKRQLQILQQSGSPVLSEDKSKRLNSIL 120
R.ferrumequinum  61:KMDEAGAKWSDFYEKQSKLAKNFSLEEIHNDTVKLQLQILQQSGSPVLSEDKSKRLNSIL 120
R.sinicus        61:KMDEAGAKWSAFYEEQSKLAKNYSLEQIQNVTVKLQLQILQQSGSPVLSEDKSKRLNSIL 120
human            61:NMNNAGDKWSAFLKEQSTLAQMYPLQEIQNLTVKLQLQALQQNGSSVLSEDKSKRLNTIL 120
                    .*..**.***.*...**..*... *..*.. .**.***.***.**.***********.**

R.cornutus      121:NAMSTIYSTGKVCKPNNPQECLLLEPGLDNIMGTSKDYHERLWAWEGWRAEVGKQLRPLY 180
R.ferrumequinum 121:NAMSTIYSTGKVCKPNNPQECLLLEPGLDNIMGTSKDYNERLWAWEGWRAEVGKQLRPLY 180
R.sinicus       121:NAMSTIYSTGKVCKPNKPQECLLLEPGLDNIMGTSKDYNERLWAWEGWRAEVGKQLRPLY 180
human           121:NTMSTIYSTGKVCNPDNPQECLLLEPGLNEIMANSLDYNERLWAWESWRSEVGKQLRPLY 180
                    *.***********.*..***********..**..*.**.*******.**.**********

R.cornutus      181:EEYVVLKNEMARGYHYEDYGDYWRRDYETEESSGPGYSRDQLMKDVDRIFTEIKPLYEHL 240
R.ferrumequinum 181:EEYVVLKNEMARGYHYEDYGDYWRRDYETEGSPDLEYSRDQLIKDVERIFAEIKPLYEQL 240
R.sinicus       181:EEYVVLKNEMARGYHYEDYGDYWRRDYETEESPGPGYSRDQLMKDVERIFTEIKPLYEHL 240
human           181:EEYVVLKNEMARANHYEDYGDYWRGDYEVNGVDGYDYSRGQLIEDVEHTFEEIKPLYEHL 240
                    ************..**********.***.. . .  ***.** .**...* *******.*

R.cornutus      241:HAYVRAKLMDTYPLHISPTGCLPAHLLGDMWGRFWTNLYPLTVPFGQKPNIDVTDEMVKQ 300
R.ferrumequinum 241:HAYVRTKLMDTYPFHISPTGCLPAHLLGDMWGRFWTNLYPLTVPFGQKPNIDVTDAMLNQ 300
R.sinicus       241:HAYVRAKLMDTYPFHISPTGCLPAHLLGDMWGRFWTNLYPLTVPFGQKPNIDVTDEMLKQ 300
human           241:HAYVRAKLMNAYPSYISPIGCLPAHLLGDMWGRFWTNLYSLTVPFGQKPNIDVTDAMVDQ 300
                    *****.***..** .***.********************.*************** *  *

R.cornutus      301:GWDANRIFKEAEKFFVSVGLPNMTEGFWNNSMLTEPGDGRKVVCHPTAWDLGKGDFRIKM 360
R.ferrumequinum 301:NWDAKRIFKEAEKFFVSIGLPNMTEGFWNNSMLTDPGDGRKVVCHPTAWDLGKGDFRIKM 360
R.sinicus       301:GWDADRIFKEAEKFFVSVGLPNMTEGFWNNSMLTEPGDGRKVVCHPTAWDLGKGDFRIKM 360
human           301:AWDAQRIFKEAEKFFVSVGLPNMTQGFWENSMLTDPGNVQKAVCHPTAWDLGKGDFRILM 360
                     *** ************.******.***.***** **...*.****************.*

R.cornutus      361:CTKVTMEDFLTAHHEMGHIQYDMAYASQPYLLRNGANEGFHEAVGEVMSLSVATPKHLKT 420
R.ferrumequinum 361:CTKVTMEDFLTAHHEMGHIQYDMAYASQPYLLRNGANEGFHEAVGEVMSLSVATPKHLKT 420
R.sinicus       361:CTKVTMEDFLTAHHEMGHIQYDMAYASQPYLLRNGANEGFHEAVGEVMSLSVATPKHLKT 420
human           361:CTKVTMDDFLTAHHEMGHIQYDMAYAAQPFLLRNGANEGFHEAVGEIMSLSAATPKHLKS 420
                    ******.*******************.**.****************.****.*******.

R.cornutus      421:MGLLSPDFREDDETEINFLLKQALNIVGTLPFTYMLEKWRWMVFKGEIPKEEWMKKWWEM 480
R.ferrumequinum 421:MGLLSSDFLEDNETEINFLFKQALNIVGTLPFTYMLEKWRWMVFKGEIPKEEWMKKWWEM 480
R.sinicus       421:MGLLSPDFREDNETEINFLLKQALNIVGTLPFTYMLEKWRWMVFKGEIPKEEWMKKWWEM 480
human           421:IGLLSPDFQEDNETEINFLLKQALTIVGTLPFTYMLEKWRWMVFKGEIPKDQWMKKWWEM 480
                    .****.** **.*******.****.************************..********

R.cornutus      481:RREIVGVVEPVPHDETYCDPASLFHVANDYSFIRYYTRTIFEFQFHEALCRIAQHNGPLH 540
R.ferrumequinum 481:KRKIVGVVEPVPHDETYCDPASLFHVANDYSFIRYYTRTIFEFQFHEALCRIAKHDGPLH 540
R.sinicus       481:KRKIVGVVEPVPHDETYCDPASLFHVANDYSFIRYYTRTIFEFQFHEALCRIAQHDGPLH 540
human           481:KREIVGVVEPVPHDETYCDPASLFHVSNDYSFIRYYTRTLYQFQFQEALCQAAKHEGPLH 540
                    .* **********************.************...***.****..* * ****

R.cornutus      541:KCDISNSTDAGKKLHQMLSVGKSQAWTKTLEDIVGSRNMDVGPLLRYFEPLYTWLQEQNR 600
R.ferrumequinum 541:KCDISNSTDAGEKLHQMLSVGKSQPWTSVLKDFVGSKNMDVGPLLRYFEPLYTWLTEQNR 600
R.sinicus       541:KCDISNSTDAGKKLHQMLSVGKSQAWTKTLEDIVDSRNMDVGPLLKYFEPLYTWLQEQNR 600
human           541:KCDISNSTEAGQKLFNMLRLGKSEPWTLALENVVGAKNMNVRPLLNYFEPLFTWLKDQNK 600
                    ********.** **..**..***. **  *.. *.. **.*.*** *****.*** .**.

R.cornutus      601:KSYVGWNTDWSPYSDQSIKVRISLKSALGEKAYEWNDNEMYLFRSSVAYAMREYFLKTKN 660
R.ferrumequinum 601:KSFVGWNTDWSPYADQSIKVRISLKSALGEKAYEWNNNEMYLFRSSVAYAMREYFLKTKN 660
R.sinicus       601:KSYVGWNTDWSPYSDQSIKVRISLKSALGENAYEWNDNEMYLFRSSVAYAMREYFLKEKH 660
human           601:NSFVGWSTDWSPYADQSIKVRISLKSALGDKAYEWNDNEMYLFRSSVAYAMRQYFLKVKN 660
                    .* ***.****** ***************..*****.***************.**** *.

R.cornutus      661:QTILFGDENVWVSNLKPRISFNFHVTSPENVSDIIPRSEVEGAIRMSRSRINDAFRLDDN 720
R.ferrumequinum 661:QTILFGEEDVWVSNLKPRISFNFYVTSPRNLSDIIPKPEVEGAIRMSRSRINDAFRLDDN 720
R.sinicus       661:QTILFGAENVWVSNLKPRISFNFHVTSPGNLSDIIPRPEVEGAIRMSRSRINDAFRLDDN 720
human           661:QMILFGEEDVRVANLKPRISFNFFVTAPKNVSDIIPRTEVEKAIRMSRSRINDAFRLNDN 720
                    *.**** * *.*.********** **.* * *****. ***.***************.**

R.cornutus      721:SLEFLGIQPTLGPPYQPPVTIWLIVFGVVMAVVVVGIVVLIITGIRDRRKTDQARSEENP 780
R.ferrumequinum 721:SLEFLGIQPTLGPPYQPPVTIWLIVFGVVMAVVVVGIVVLIITGIRDRRKKDQARSEENP 780
R.sinicus       721:SLEFLGIQPTLGPPYQPPVTIWLIVFGVVMAVVVVGIVVLIITGIRDRRKTDQARSEENP 780
human           721:SLEFLGIQPTLGPPNQPPVSIWLIVFGVVMGVIVVGIVILIFTGIRDRKKKNKARSGENP 780
                    *************.****.**********.*.*****.**.******.* ..***.***

R.cornutus      781:YPSVDLSKGENNPGFQNGDDVQTSF                                    805
R.ferrumequinum 781:YSSVDLSKGENNPGFQNGDDVQTSF                                    805
R.sinicus       781:YSSVDLSKGENNPGFQNGDDVQTSF                                    805
human           781:YASIDISKGENNPGFQNTDDVQTSF                                    805
                    * *.*.***********.*******
```

Appendix Figure 2. Alignment of ACE2 amino acid sequence from *Rhinolophus cornutus*, *R. ferrumequinum*, *R. sinicus,* and humans. Deduced amino acid sequence of *R. cornutus* ACE2 RNA was aligned with those of *R. ferrumequinum, R. sinicus,* and human ACE2. Highlighted yellow region was considered the spike protein binding region of *R. cornutus* ACE2. ACE2, angiotensin-converting enzyme 2.

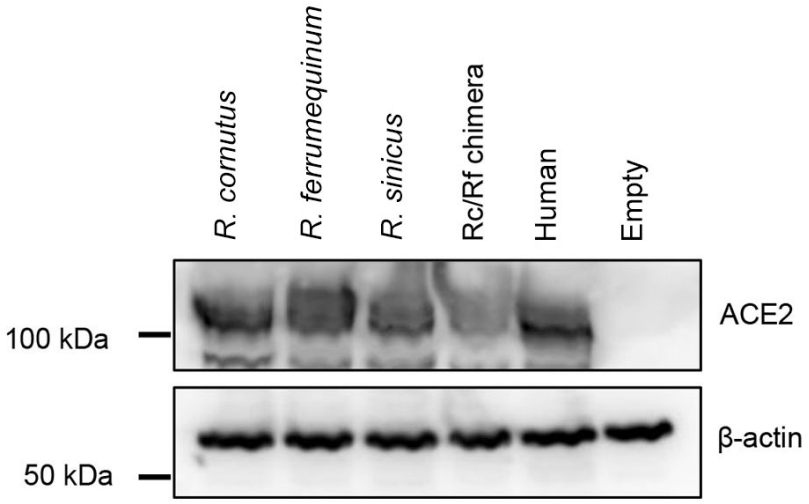

Appendix Figure 3. Western blot analysis showing expression of angiotensin-converting enzyme 2 in transfected cells from bats and humans. HEK293T cells that transiently expressed *Rhinolophus cornutus*, *R. ferrumequinum*, *R. sinicus*, Rc/Rf chimera (spike protein [S] interaction domain from *R. cornutus* and the remaining from *R. ferrumequinum*), or human ACE2. ACE2, angiotensin-converting enzyme 2; HEK293T cells, human embryonic kidney 293T cells.

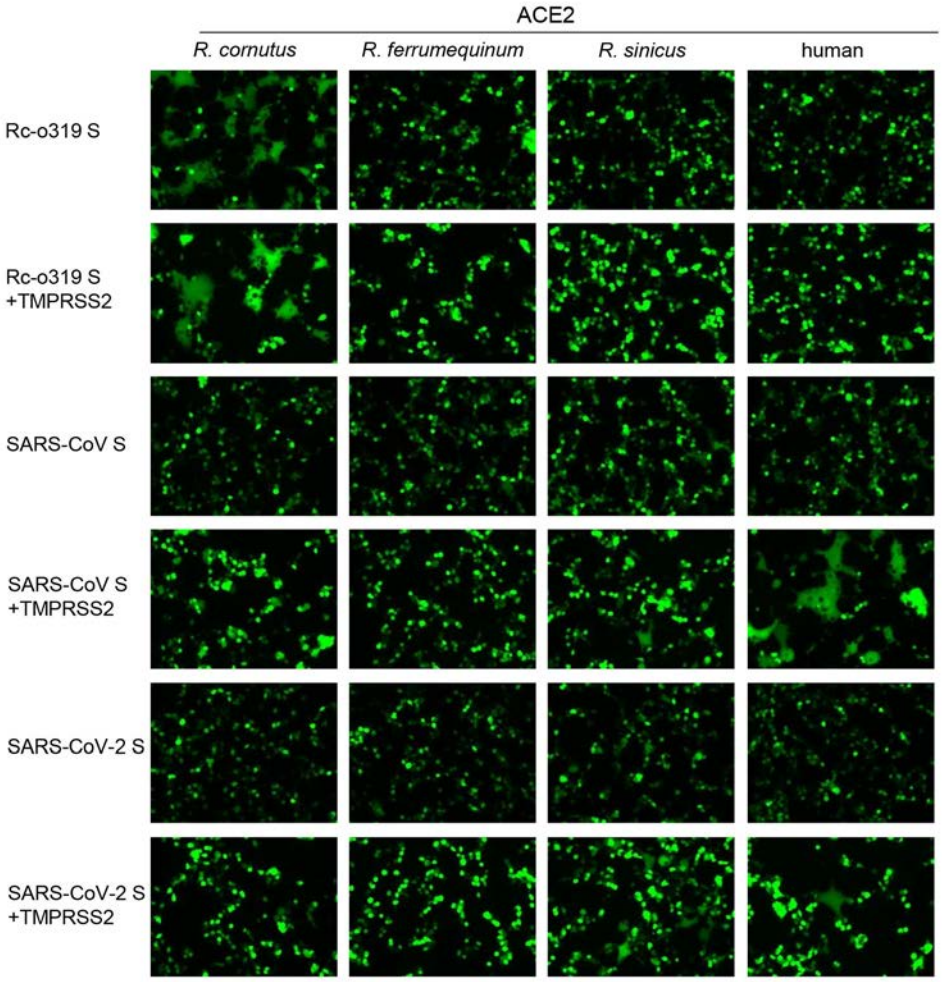

Appendix Figure 4. Results of fusion assay in which HEK293T cells were cotransfected with S-expression plasmids and ACE2 from bat and human sarbecoviruses. S-expression plasmids of Rc-o319, SARS-CoV, or SARS-CoV-2 and expression plasmids of Rc-ACE2, Rf-ACE2, Rs-ACE2, or hACE2, and fluorescent reporter Venus-expression plasmid with and without TMPRSS2-expression plasmid were incubated for 24 h to assess syncytium formation. At 24 h post-transfection, the cells were observed under a fluorescence microscope. ACE2, angiotensin-converting enzyme 2; hACE2, human ACE2; HEK293T cells, human embryonic kidney 293T cells; Rc-o319, sarbecovirus identified in this study; Rc-ACE2, *Rhinolophus cornutus* ACE2; Rf-ACE2, *R. ferrumequinum* ACE2; Rs-ACE2, *R. sinicus* ACE2; S, spike glycoprotein; SARS-CoV, severe acute respiratory syndrome coronavirus; SARS-CoV-2, severe acute respiratory syndrome coronavirus 2; TMPRSS2, transmembrane serine protease 2.